Terahertz transmission in subwavelength holes of asymmetric metal-dielectric interfaces: The effect of a dielectric layer

Jiaguang Han, Xinchao Lu, and Weili Zhang[a)]
School of Electrical and Computer Engineering, Oklahoma State University, Stillwater, Oklahoma 74078, USA

(Received 9 November 2007; accepted 21 November 2007; published online 14 February 2008)

The influence of a dielectric thin film on resonant transmission of terahertz pulses in a plasmonic array of subwavelength holes of asymmetric dielectric-metal interfaces is presented. A giant tuning of up to 0.80 THz at the surface plasmon metal-air $[\pm 1,0]$ mode at 1.95 THz and a further enhanced transmission at the metal-Si $[\pm 1,0]$ mode at 0.5 THz are achieved by modifying the film thickness. The experimental results are characterized by numerical simulation based on finite element method and angle-dependent measurements. The sensitive nature in the plasmonic hole array of asymmetric interfaces is promising in applications of biochemical sensing and tunable integrated plasmonic devices. © *2008 American Institute of Physics*. [DOI: 10.1063/1.2837090]

I. INTRODUCTION

In transmission enhancement of electromagnetic waves through an array of subwavelength holes, resonant excitation of surface plasmons (SPs), originated from the periodicity of metallic structures, was demonstrated to play a substantial role.[1–12] One of the fascinating characteristics of the array is that their resonant frequencies are extremely sensitive to the dielectric function of the medium adjacent to the metal surface. This property makes such palsmonic arrays very promising in biochemical sensing applications.[13–17] In particular, arrays with asymmetric metal-dielectric interfaces on both sides, such as an air-metal-substrate system, provide improved sensitivity because the analytes ($\varepsilon > 1$) applied on the array not only replace air as a dielectric medium at the metal surface, but also fill up the hole cavities formed against the substrate. This in turn provides extensive modification of the strength and peak frequencies of the SP resonances in the array.

In this article, we present the effect of a dielectric layer on terahertz transmission through a subwavelength hole array of asymmetric metal-dielectric interfaces. Modification of the layer thicknesses leads to a significant tuning of resonant terahertz transmission at the SP modes. The metal-air SP $[\pm 1,0]$ mode at 1.95 THz exhibits up to 0.80 THz remarkable tuning range, while the peak amplitude transmission of the metal-Si SP $[\pm 1,0]$ mode at 0.5 THz is enhanced from 0.82 to 0.94, due to resulted change in wave vectors of the SP modes by the dielectric overlayer. The experimental results are analyzed by angle-resolved measurements and a frequency domain finite element method (FEM) simulation.

II. EXPERIMENTS

To prepare the sample, a 180 nm thick Al array of subwavelength rectangular holes is lithographically fabricated on a silicon wafer (0.64 mm thick, *p*-type resistivity 20 Ω cm).[18–20] The dimensions of the holes are 80 μm (x axis) $\times$ 100 μm (y axis) with a lattice period of 160 μm as illustrated in the inset of Fig. 1. A dielectric layer made from photoresist ($\varepsilon_2 = 2.2 \pm 0.1$ at 1.1 THz, Futurrex, Inc.) is spin-coated on the 25×25 mm^2 sized array by a single-wafer spin processor (Laurell WS-400A). Terahertz time-domain spectroscopy (THz-TDS) transmission measurement is employed to characterize the resonant properties of the array.[21] The photoconductive switch-based THz-TDS system consists of four paraboloidal mirrors arranged in an 8-F confocal geometry. This configuration enables excellent terahertz beam coupling between the transmitter and receiver and compresses the beam to a frequency-independent beam waist with a diameter of 3.5 mm as well. The THz-TDS system has a usable bandwidth of 0.1–4.5 THz (3 mm to

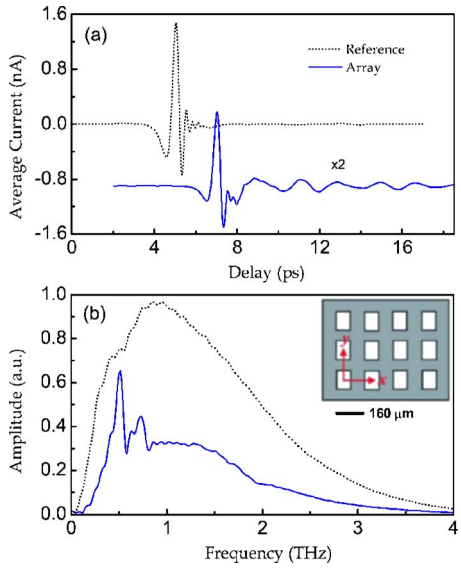

FIG. 1. (Color online) (a) Measured terahertz pulses transmitted through the reference and the array without the dielectric overlayer. For clarity, the pulses are displaced by 0.9 nA vertically and 2 ps horizontally. (b) Corresponding Fourier-transformed amplitude spectra. Inset: Schematic diagram of the array of subwavelength holes of dimensions 80 μm (x axis) $\times$ 100 μm (y axis).

[a)]Author to whom correspondence should be addressed. Electronic mail: wwzhang@okstate.edu.

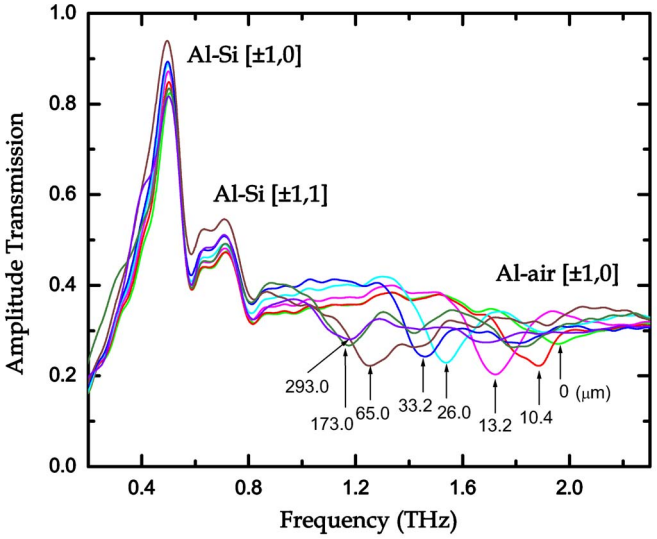

FIG. 2. (Color online) Amplitude transmission of terahertz pulses in a Al subwavelength hole array with a dielectric overlayer of different thicknesses varying from 0 to 293 μm.

67 μm) and a signal to noise ratio (S/N) of >15 000:1.[20,22] To carry out far-field terahertz characterization, the array is placed midway between the transmitter and receiver modules at the waist of the terahertz beam. The polarization of the terahertz electric field is perpendicular to the longer axis ($E \perp y$) of the holes.

III. RESULTS AND DISCUSSION

Figure 1 shows the measured terahertz pulses and the corresponding Fourier-transformed amplitude spectra transmitted through a reference and the array without the dielectric overlayer. The reference is a blank silicon slab identical to the array substrate. In order to further improve the S/N of THz-TDS measurements, each curve is an average of six individual scans. The extracted frequency-dependent amplitude transmission of the array with a dielectric overlayer of various thicknesses d, from 0 to 293 μm, is illustrated in Fig. 2. The transmission is defined as $T(\omega) = |E_{\text{out}}(\omega)/E_{\text{in}}(\omega)|$, where $E_{\text{out}}(\omega)$ and $E_{\text{in}}(\omega)$ are amplitudes of the terahertz pulses through the array and reference, respectively; the latter is spin-coated with the same dielectric overlayer as that on the array sample. As indicated by the arrows, the SP resonance of the Al-air $[\pm 1,0]$ mode drops to lower frequencies with increasing d, whereas the resonance frequencies of the Al-Si $[\pm 1,0]$ and $[\pm 1,1]$ modes reveal only minor redshifts. Without the dielectric layer, the resonance of the Al-air $[\pm 1,0]$ mode occurs at 1.95 THz; while it shifts to 1.87 THz with a layer thickness of 10.4 μm. When the dielectric film is getting thicker up to 65 μm, this resonance redshifts significantly to 1.25 THz. Further increase in layer thickness, however, leads to a little variation at this resonance mode, and it is eventually saturated at 1.17 THz with layer thicknesses varying from 173 to 293 μm. In addition, the peak amplitude transmission at the SP modes is modified by the dielectric overlayer as well.

In a metal array, SPs can be resonantly excited at the metal-dielectric interfaces following momentum conservation,[5,23,24]

$$\mathbf{k_{sp}} = \mathbf{k}_{\parallel} + m\mathbf{G_x} + n\mathbf{G_y}, \tag{1}$$

where $\mathbf{k_{sp}}$ is the wave vector of SPs, $\mathbf{k}_{\parallel}$ is the in-plane wave vector, $\mathbf{G_x}$ and $\mathbf{G_y}$ are the reciprocal lattice vectors, $G_x = G_y = 2\pi/L$ for a square-lattice, and m and n are integers. The remarkable shift in the resonant frequency at the Al-air $[\pm 1,0]$ SP mode due to the addition of the dielectric layer can be understood through the dispersion relation of the SP modes at normal incidence,[5,23,24]

$$k_{\text{sp}} = \frac{\omega}{c}\text{Re}\left(\frac{\varepsilon_d \varepsilon_m}{\varepsilon_d + \varepsilon_m}\right)^{1/2}, \tag{2}$$

where ε_m and ε_d denote the dielectric function of metal and the adjacent dielectric medium, respectively. In our case, without the dielectric layer, the adjacent medium is air, giving $\varepsilon_d = \varepsilon_1 = 1$. When the dielectric film is applied on metal surface and if the film thickness $d > \lambda$ is fulfilled, with λ the resonance wavelength, the dispersion in Eq. (2) can be modified from $k_{\text{sp}}(\varepsilon_d = \varepsilon_1)$ to $k_{\text{sp}}(\varepsilon_d = \varepsilon_2)$, where ε_2 is the dielectric function of the overlayer film, as shown in the inset of Fig. 3. Thus, the resonant frequency shifts due to modification of the dielectric function of the adjacent medium. When the overlayer thickness is less than the resonance wavelength $d < \lambda$, however, the dielectric layer ε_2 along with the ambient air ε_1 serve as an effective adjacent medium to the metal. The shift in SP resonance arises from the modification of the SP wave vector due to a thickness change of the overlayer.[25]

In the terahertz regime, the frequency-dependent dielectric function of Al can be described by the Drude model, $\varepsilon_m = \varepsilon_c - \omega_p^2/(\omega^2 + i\gamma\omega)$.[26] At 1.0 THz, $\varepsilon_{\text{Al}} = -3.37 \times 10^4 + 6.62 \times 10^5 i$. Since $\varepsilon_m = \varepsilon_{\text{Al}} \gg \varepsilon_2$, the modified wave vector of SPs due to the existence of the dielectric overlayer is approximately given as terahertz frequencies as

$$k_{\text{sp}} \approx \frac{\omega}{c}\left\{1 + \left[\frac{1}{2}\left(\frac{\varepsilon_2 - 1}{\varepsilon_2}\right)^2\right]s^2\right\}, \tag{3}$$

where $s = \omega d/c$ and c is the light speed.[25] Thus, by combining Eqs. (1) and (3), the SP resonant frequency at the Al-air $[\pm 1,0]$ mode as a function of the overlayer thickness can be calculated, as shown by the solid curve in Fig. 3. Being consistent with the measured results, the theoretical values of the resonant frequency drop rapidly with increasing film thickness up to 65 μm. Beyond 65 μm, however, the calculated resonant frequency shows discrepancy with the measured data. This is due to the existence of a critical dielectric film thickness, $d_c = \lambda/4(\varepsilon_2 - 1)^{1/2}$; at 1.1 THz, $d_c \approx 63$ μm.[25] When the film thickness $d > d_c$, Eq. (3) is no longer valid, and the resonant frequency shows a slow variation with film thickness and eventually approaches a constant. In this case, the SP resonance can be evaluated solely at the Al-dielectric layer (ε_2) interface through the relation $k_{\text{sp}} = (\omega/c)\varepsilon_2^{1/2}$.[18]

To achieve an in-depth understanding of the effect of the dielectric layer on SP resonance properties, an angle-resolved transmission measurement is carried to reveal a full band structure of the plasmonic array. The in-plane wave

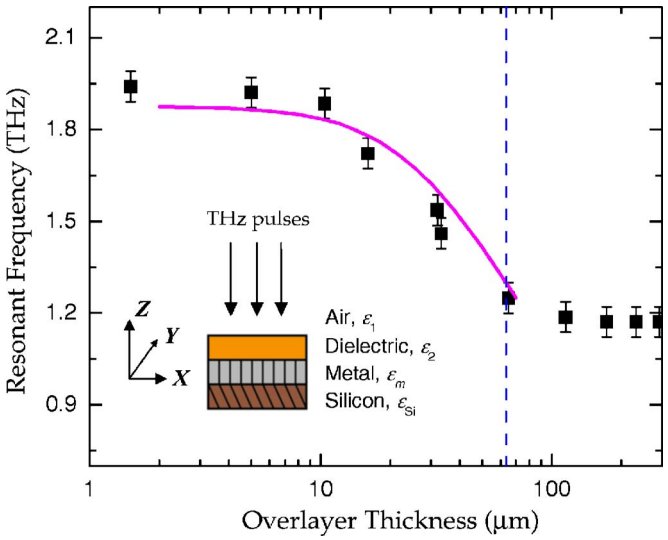

FIG. 3. (Color online) Resonant frequencies of the Al-air $[\pm 1,0]$ mode as a function of the thickness of the overlayer dielectric film. Experimental data: squares; numerical calculation: solid curve. Inset: schematic of the metal-dielectric interfaces of the array system.

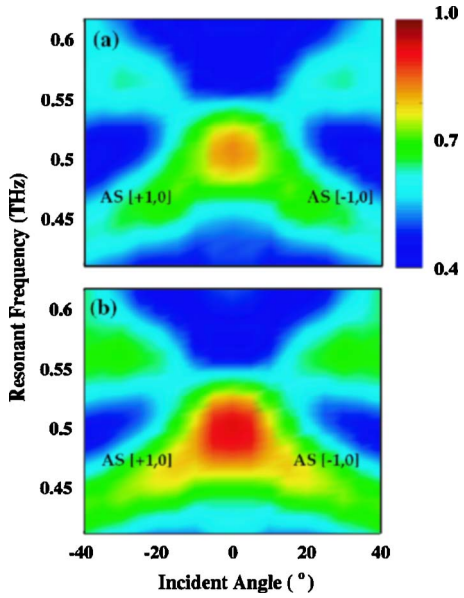

FIG. 5. (Color online) Angle-resolved transmission of the Al-Si (AS) $[\pm 1,0]$ mode without (a) and with (b) the 65 μm thick dielectric overlayer.

vector $k_{\parallel}$ shown in Eq. (1) is a component of the incident wave vector k_0 in the array plane, defined as $k_{\parallel}=(\omega/c)\sin\theta$, where θ is the incidence angle. Hence, the resonant frequency of the excited SP mode can be continuously tuned by varying the angle of incidence. Figures 4(a) and 4(b) illustrate the full band structures of the Al-air $[\pm 1,0]$ SP mode without and with the 65 μm thick dielectric overlayer, respectively, with the incidence angle varied from −40° to 40°. The amplitude transmission is plotted in the (f,θ) plane with a color scale proportional to the magnitude. The influence of the overlayer on SP resonance properties is clearly observed. The full band of the Al-air $[\pm 1,0]$ SP mode is shifted toward lower frequencies when the 65 μm thick dielectric layer is applied on the array surface.

It is also of interest to note that the amplitude transmission at the Al-air $[\pm 1,0]$ SP mode reveals only a minor change with the overlayer thickness, with a minimum around a level of 0.25. This is because the dielectric layer is nearly transparent at terahertz frequencies and the damping term in this layer is negligible ($\varepsilon_2''=0$).[23,24,27] While the dielectric film leads to a redshift in the SP band at the Al-air interface, it also shows a quite distinct influence on the fundamental SP resonance mode at the Al-Si interface.

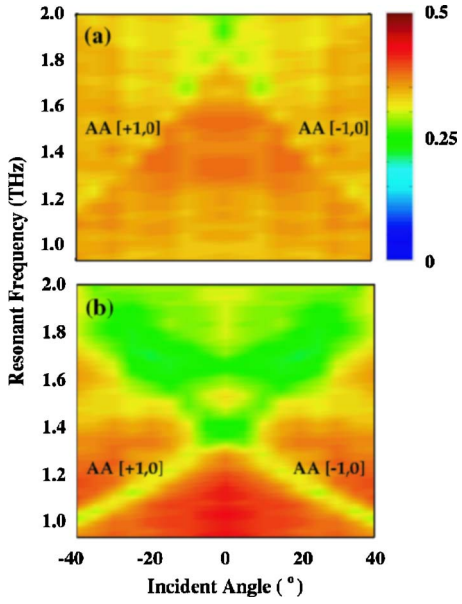

FIG. 4. (Color online) Angle-resolved transmission of the Al-air (AA) $[\pm 1,0]$ mode without (a) and with (b) the 65 μm thick dielectric overlayer.

As shown in Fig. 2, the presence of the dielectric layer gives rise to an enhancement in resonant transmission at the Al-Si $[\pm 1,0]$ 0.5 THz mode. With the 65 μm thick overlayer, the peak amplitude transmission increases from 0.82 to 0.94 at normal incidence, but it rarely affects the resonant frequency. The full band structure of the Al-Si $[\pm 1,0]$ mode with the overlayer remains nearly unchanged compared to that of the bare metal array, except for the increase in transmission strength, as shown in Fig. 5. This is because the resonant frequency of SPs at the Al-Si interface is directly related to the dispersion relation described by Eq. (2) with $\varepsilon_d=\varepsilon_{Si}$, the dielectric function of silicon substrate, and the dielectric function of the overlayer does not make a direct contribution to the resonant frequency of the Al-Si $[\pm 1,0]$ mode. However, the modification of resonance amplitude with the dielectric layer is interesting. The observed increase in resonant transmission at the Al-Si $[\pm 1,0]$ mode suggests that there exists an enhanced electric field at the interface due to the presence of the 65 μm thick dielectric layer.

A further verification is provided by examining the modeled field distribution at the array interfaces. At 0.5 THz, the peak resonance of the Al-Si $[\pm 1,0]$ mode, the electric field vector is simulated using frequency domain FEM for normal incidence, as illustrated in Figs. 6(a) and 6(b), respectively, without and with the 65 μm thick overlayer. The arrows point at the direction of electric field **E** and the colors are proportional to the magnitude of the electric field. The field-line loops are enhanced noticeably into the hole due to addition of the dielectric layer as compared to that of the bare

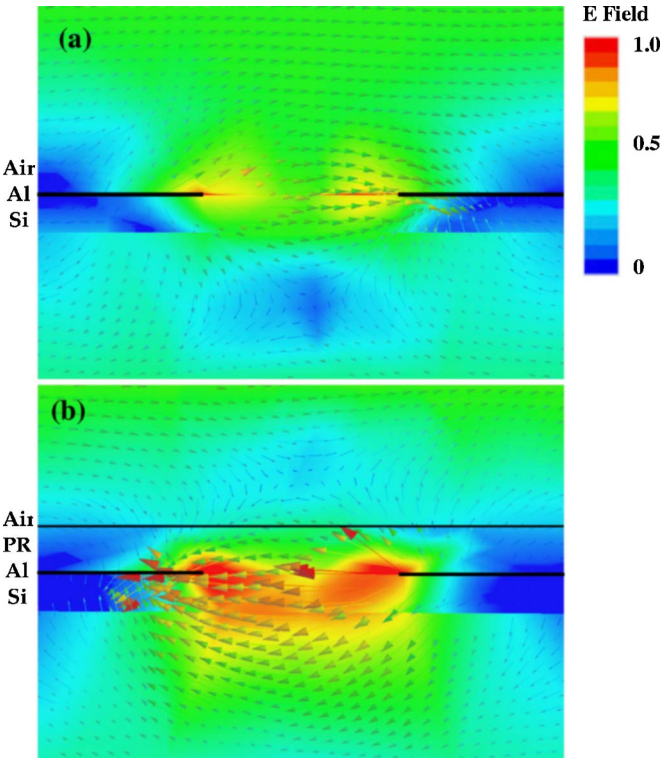

FIG. 6. (Color online) Comparison of modeled electric field by FEM at 0.5 THz, the Al-Si (AS) $[\pm 1,0]$ mode, without (a) and with (b) the 65 μm thick dielectric overlayer.

array. The appropriate dielectric overlayer of $\varepsilon_2 > \varepsilon_1$ indeed results in the increased coupling of the terahertz wave into SPs at the dielectric-Al $(\varepsilon_2 - \varepsilon_m)$ interface.

IV. CONCLUSION

In conclusion, the dielectric overlayer on the subwavelength hole array of asymmetric metal-dielectric interfaces has shown a strong influence on resonant terahertz transmission due to modification of wave vectors of the SP modes. With various thicknesses of the overlayer, the Al-air SP $[\pm 1,0]$ mode exhibits a large tuning range, while the peak amplitude transmission of the low-frequency Al-Si SP $[\pm 1,0]$ mode is enhanced noticeably. This finding is very promising in on-chip terahertz sensing of biological and chemical agents, as well as tuning and modification of resonant frequencies of plasmonic terahertz devices.

ACKNOWLEDGMENTS

The authors acknowledge fruitful discussions with F. He, K. Ji, and Z. Y. Zhu. This work was partially supported by the National Science Foundation. J.G.H. is now with the National University of Singapore.

[1] T. W. Ebbesen, H. J. Lezec, H. F. Ghaemi, T. Thio, and P. A. Wolff, Nature (London) **391**, 667 (1998).
[2] W. L. Barnes, A. Dereux, and T. W. Ebbesen, Nature (London) **424**, 824 (2003).
[3] L. Martín-Moreno, F. J. García-Vidal, H. J. Lezec, A. Degiron, and T. W. Ebbesen, Phys. Rev. Lett. **90**, 167401 (2003).
[4] K. J. Klein Koerkamp, S. Enoch, F. B. Segerink, N. F. van Hulst, and L. Kuipers, Phys. Rev. Lett. **92**, 183901 (2004).
[5] H. F. Ghaemi, T. Thio, D. E. Grupp, T. W. Ebbesen, and H. J. Lezec, Phys. Rev. B **58**, 6779 (1998).
[6] E. Ozbay, Science **311**, 189 (2006).
[7] G. Torosyan, C. Rau, B. Pradarutti, and R. Beigang, Appl. Phys. Lett. **85**, 3372 (2004).
[8] J. Saxler, J. G. Rivas, C. Janke, H. P. M. Pellemans, P. H. Bolivar, and H. Kurz, Phys. Rev. B **69**, 155427 (2004).
[9] H. Cao and A. Nahata, Opt. Express **12**, 1004 (2004).
[10] J. O'Hara, R. D. Averitt, and A. J. Taylor, Opt. Express **12**, 6397 (2004).
[11] J. B. Masson and G. Gallot, Phys. Rev. B **73**, 121401(R) (2006).
[12] W. Zhang, A. K. Azad, J. Han, J. Xu, J. Chen, and X.-C. Zhang, Phys. Rev. Lett. **98**, 183901 (2007).
[13] A. G. Brolo, R. Gordon, B. Leathem, and K. K. Kavanagh, Langmuir **20**, 4813 (2004).
[14] J. Dintinger, S. Klein, F. Bustos, W. L. Barnes, and T. W. Ebbesen, Phys. Rev. B **71**, 035424 (2005).
[15] S. M. Williams, K. R. Rodriguez, S. Teeters-Kennedy, A. D. Stafford, S. R. Bishop, U. K. Lincoln, and J. V. Coe, J. Phys. Chem. B **108**, 11833 (2004).
[16] M. Tanaka, F. Miyamaru, M. Hangyo, T. Tanaka, M. Akazawa, and E. Sano, Opt. Lett. **30**, 1210 (2005).
[17] F. Miyamaru, S. Hayashi, C. Otani, K. Kawase, Y. Ogawa, H. Yoshida, and E. Kato, Opt. Lett. **31**, 1118 (2006).
[18] D. Qu, D. Grischkowsky, and W. Zhang, Opt. Lett. **29**, 896 (2004).
[19] D. Qu and D. Grischkowsky, Phys. Rev. Lett. **93**, 196804 (2004).
[20] A. K. Azad and W. Zhang, Opt. Lett. **30**, 2945 (2005).
[21] D. Grischkowsky, S. Keiding, M. Van Exter, and Ch. Fattinger, J. Opt. Soc. Am. B **7**, 2006 (1990).
[22] A. K. Azad, Y. Zhao, and W. Zhang, Appl. Phys. Lett. **86**, 141102 (2005).
[23] H. Raether, *Surface Plasmons on Smooth and Rough Surfaces and on Gratings* (Springer-Verlag, Berlin, 1988).
[24] V. M. Agranovich and D. L. Mills, *Surface Polaritons* (North-Holland, New York, 1982).
[25] Z. Schlesinger and A. J. Sievers, Phys. Rev. B **26**, 6444 (1982).
[26] M. A. Ordal, L. L. Long, R. J. Bell, S. E. Bell, R. R. Bell, R. W. Alexander, Jr., and C. A. Ward, Appl. Opt. **22**, 1099 (1983).
[27] G. J. Kovacs and G. D. Scott, Phys. Rev. B **16**, 1297 (1977).